

G&G

Micro-World

Editor: Nathan Renfro

Contributing Editors: Elise A. Skalwold and John I. Koivula

Rare Blue Apatite Inclusion in Smoky Quartz

A natural smoky quartz with an obvious mineral inclusion at the center of the stone (figure 1) was recently observed by the author. Raman analysis confirmed that this mineral was apatite. The apatite had very light blue color and a hexagonal twinned morphology. Under cross-polarized light, the inclusion showed interference colors, confirming its doubly refractive nature (figure 2).

Apatite is a phosphate mineral with the chemical formula of $\text{Ca}_5(\text{PO}_4)_3(\text{Cl}/\text{F}/\text{OH})$. Generally, smoky quartz and apatite can occur under the same geologic conditions, including pegmatitic hydrothermal environments. Apatite is commonly a protogenetic inclusion, but it can occasionally result from a later stage and be considered a syngenetic inclusion in quartz. The rounded shape of this apatite example suggests a protogenetic inclusion, one that would be a welcome sight for any gemologist examining stones in a microscope.

*Nattapat Karava
GIA, Bangkok*

Apatite Oiling: Before and After

Fissure filling of gemstones is an age-old treatment that can improve a stone's clarity (Fall 2020 Gem News International, pp. 443–444). By introducing oil or other fillers such as resin into the stone, the treater can minimize the appearance of fissures.

Recently we had the opportunity to observe this treatment up close in an apatite cabochon brought to our laboratory for photography while it was still untreated. Then

About the banner: Dark exsolution stringers of magnetite show vivid interference colors using reflected light in this yellow scapolite from Tanzania. Photomicrograph by Nathan Renfro; field of view 4.08 mm. Courtesy of Arsaa Gems and Minerals.

GEMS & GEMOLOGY, VOL. 58, No. 1, pp. 62–71.

© 2022 Gemological Institute of America



Figure 1. A hexagonal apatite inclusion in smoky quartz. Photomicrograph by Nattapat Karava; field of view 6.3 mm.

the sample was oiled by Jeffery Bergman and returned to the laboratory for observation and photography.

Figure 2. A hexagonal apatite inclusion with interference colors in smoky quartz, viewed in cross-polarized illumination. Photomicrograph by Nattapat Karava; field of view 6.3 mm.



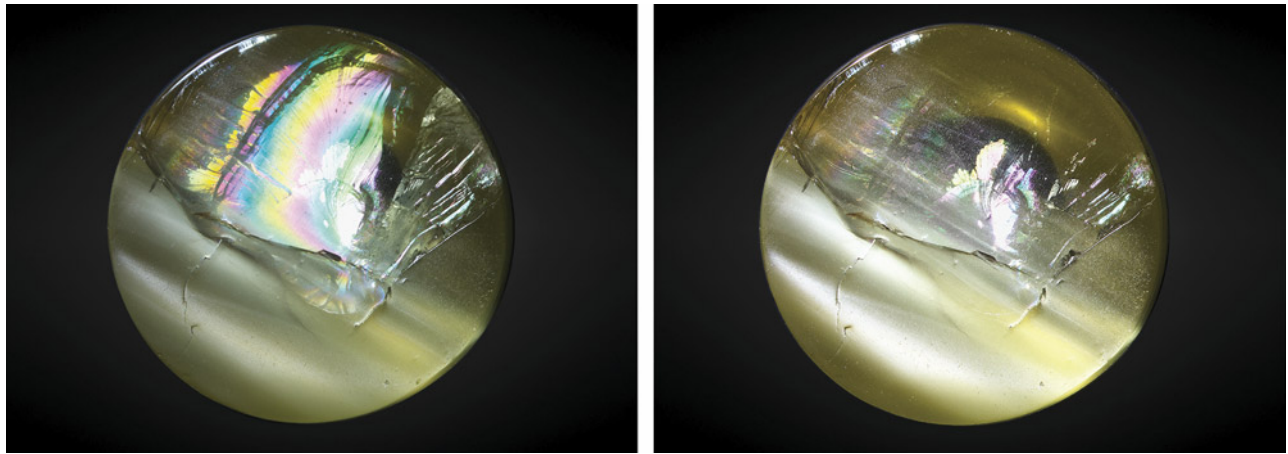


Figure 3. Left: On the base of this apatite cabochon (15 × 15 × 13 mm), a large, reflective fissure can be observed with fiber-optic illumination. Right: After the oil filling, the same fissure is much less noticeable and the iridescent reflective area is considerably smaller, enhancing the sample's clarity. Photos by E. Billie Hughes.

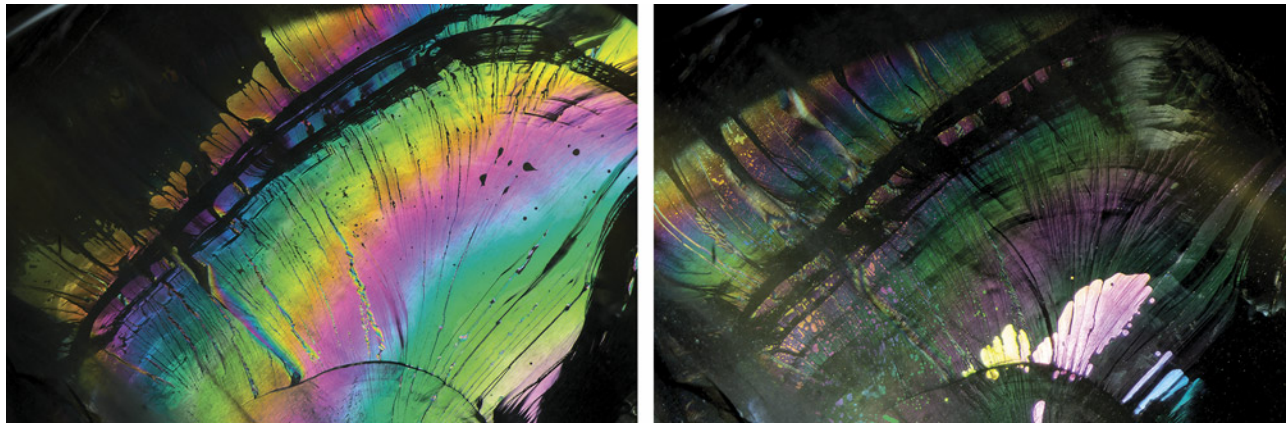


Figure 4. A close-up of the fissure before and after oil treatment, shown in diffuse fiber-optic illumination. Left: Before oiling, the fissure is easily visible and highly reflective. Right: After oiling, the reflection is more muted and less noticeable, with only a small highly reflective area remaining. Photomicrographs by E. Billie Hughes; field of view 10 mm.

Upon examination before and after, the effects of the treatment were clear. On the base of the cabochon, a large, reflective fissure became less visible after oiling (figure 3). Using fiber-optic illumination, it was apparent that the filler had diminished the reflective appearance of the fissure, with only small highly reflective areas remaining (figure 4). Darkfield illumination also revealed a stark

difference in appearance: The filler had rendered large dark areas filled with air nearly invisible (figure 5).

This microscopic observation serves as a reminder of the significant impact clarity enhancement can have on gems of all types.

E. Billie Hughes
Lotus Gemology, Bangkok

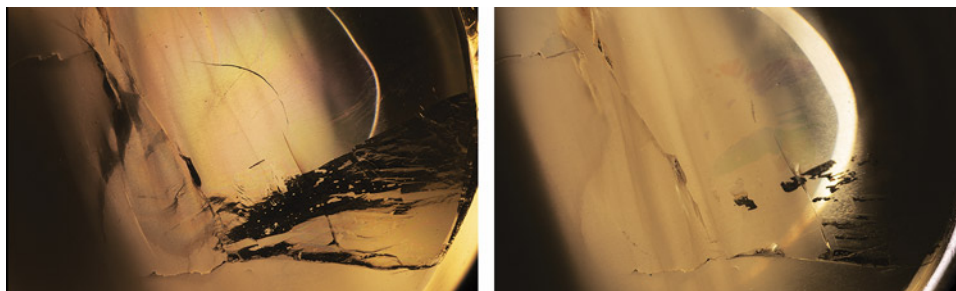


Figure 5. Left: Before filling, transmitted light shows dark areas where air has become trapped in the fissure, making it more visible. Right: Treatment with oil minimizes the dark areas, enhancing clarity. Photomicrographs by E. Billie Hughes; field of view 27 mm.

Acicular Troughs Coincident with Green Stains on Rough Diamond Surface

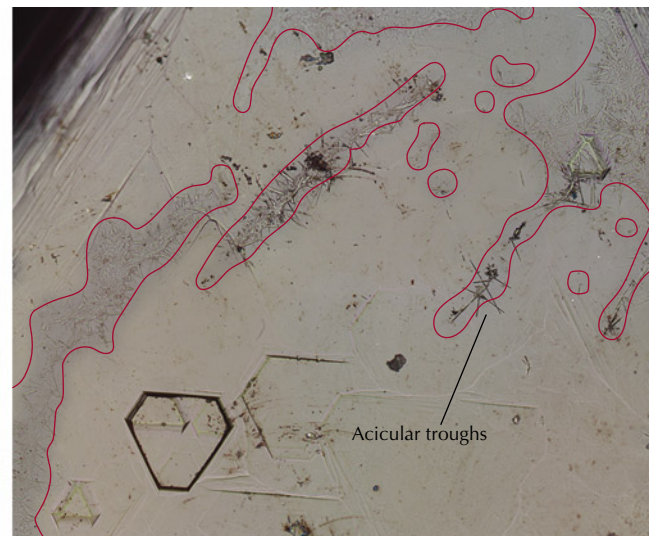
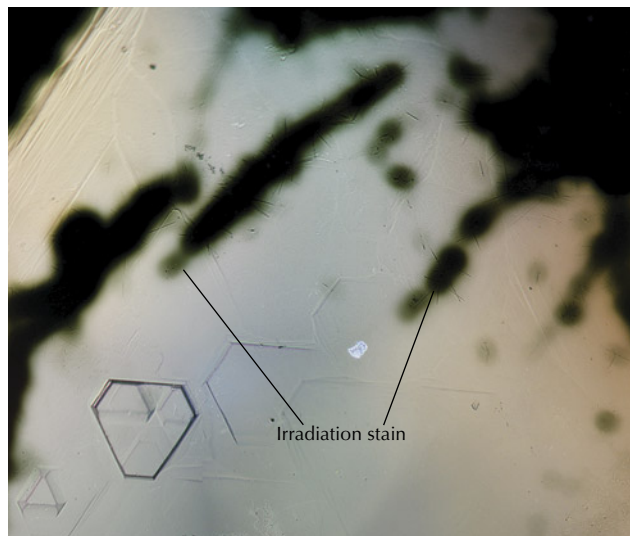
The author acquired an alluvial rough diamond from Guyana showing unique surficial features that do not appear to have been documented elsewhere. The specimen was a twinned crystal consisting of two intergrown octahedral crystals, ~0.12 ct in weight, with numerous flat-bottomed hexagonal etch features and trigons and a nearly pervasive green skin (figure 6). Most interesting were fine, linear, and randomly oriented features on the diamond surface that were spatially associated with the green stains (figure 7). Radiation stains are known to cause localized expansion in diamond (L. Nasdala et al., "Radio-coloration of diamond: A spectroscopic study," *Contributions to Mineralogy and Petrology*, Vol. 165, 2013, pp. 843–861; S.C. Eaton-Magaña and K.S. Moe, "Temperature effects on radiation stains in natural diamonds," *Diamond and Related Materials*, Vol. 64, 2016, pp. 130–142). These features also cross-cut trigons, implying that they post-date the diamond's growth in the earth's mantle and its surface dissolution within the kimberlite magma (figure 8). These features may be the result of localized dissolution caused by proximal acicular, radioactive, and as yet unknown minerals, leaving behind a cast impression. Green color in diamond can be produced by natural irradiation of the crystal lattice by exposure to radiation from proximal and adjacent radioactive grains (e.g., zircon, monzonite, uraninite, and K-feldspar) or salts dissolved in percolating fluids surrounding the diamond (C.M. Breeding et al., "Natural-color green diamonds: A beautiful conundrum," *Spring 2018 GeG*, pp. 2–27). Gamma, alpha, or beta radiation emanating from these sources are thought to cause collections of



Figure 6. A ~0.12 ct green-skinned diamond from Guyana. Photo by Roy Bassoo.

defects and impurities within the diamond. Gamma and beta radiation have low energies and long penetration depths producing green bodycolors. Due to its high energy, alpha radiation has the shortest penetration depth and only within the first 25 μm of the diamond surface, creating green skins, stains, and spots.

Figure 7. Left: A magnified view of green radiation stains on an unpolished diamond surface in transmitted light. Right: An image of the same surface in reflected light with the radiation staining (outlined in red) and preserved acicular troughs. Photomicrographs by Roy Bassoo; field of view 0.5 mm.



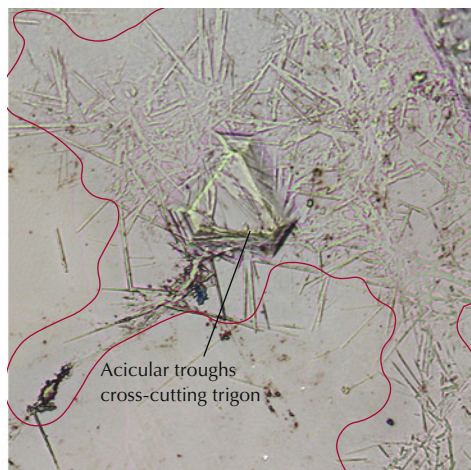
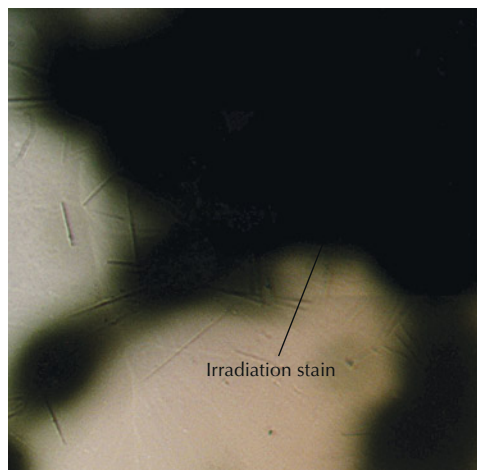


Figure 8. A further magnified view of the green radiation stains on an unpolished diamond surface in transmitted light (left) and an image of the same surface in reflected light with the radiation staining outlined in red and preserved acicular troughs which cross-cut a flat-bottomed trigon (right). Photomicrographs by Roy Bassoo; field of view 0.25 mm.

Although unusual, radiation-related surface features have been previously documented (e.g., Spring 2021 *G&G Micro-World*, pp. 66–67). The ones seen in this diamond from Guyana appear to be unique, however. It is quite likely that these features are pervasive in placer diamonds but have not been studied in detail.

Roy Bassoo
GIA, Carlsbad

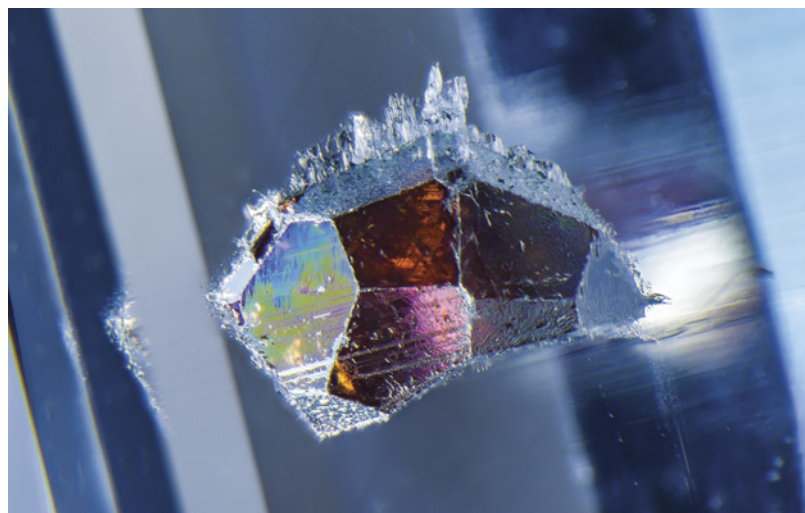
Figure 9. A 7.98 ct blue aquamarine faceted by the author to display the garnet crystal within. Photo by Jessa Rizzo.



Spessartine Garnet in Aquamarine

The author recently had the opportunity to examine and facet a sample of aquamarine rough. The aquamarine, reportedly from Pakistan, was acquired from gemstone dealer Ali Shad of Shad Fine Minerals (Gilgit-Baltistan, Pakistan). The rough was specifically selected for the large red garnet inclusion within. In preparation for faceting, the stone was oriented with the garnet inclusion as the primary focus. After careful planning and execution, a 7.98 ct modified emerald cut was achieved, highlighting the garnet crystal under the table facet (figure 9). Oblique fiber-optic illumination was used to observe the internal features of the aquamarine, revealing a well-formed red spessartine garnet crystal with iridescent colors along the garnet and aquamarine interface (figure 10). This is one of the most

Figure 10. The red spessartine garnet showed vibrant interference colors along the interface with the aquamarine host. Photomicrograph by Nathan Renfro; field of view 5.63 mm.



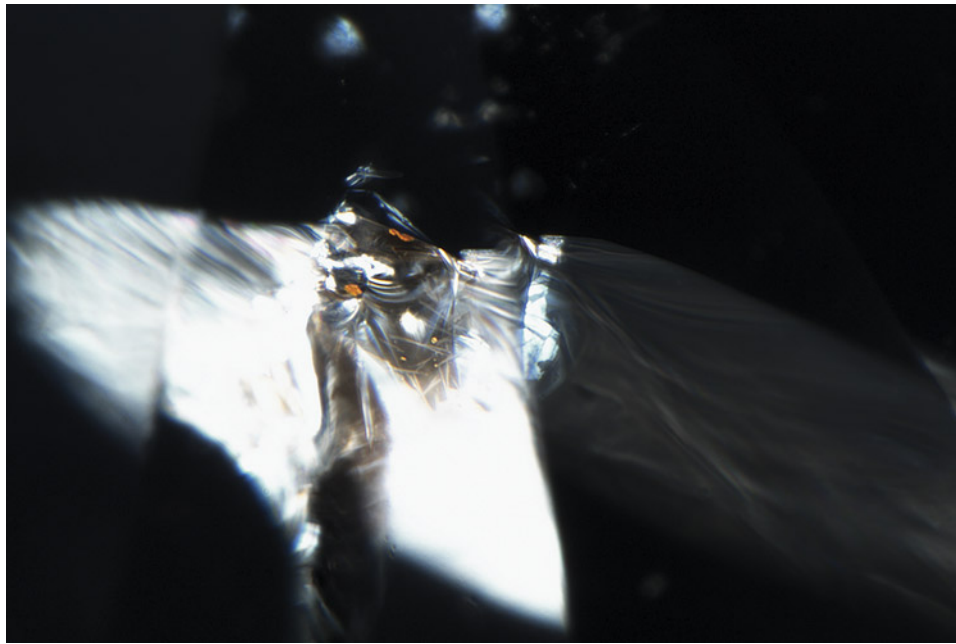


Figure 11. Several small brownish orange crystals found within the fracture of a diamond were identified as hematite. Photomicrograph by Abadie Ludlam; field of view 1.26 mm.

beautiful inclusions the author has seen in an aquamarine, and it is noteworthy as the gem was faceted to display the inclusion rather than to conceal or remove it.

Jessa Rizzo
GIA, Carlsbad

Hematite Crystals in Diamond

A 1.51 ct G-color diamond with I₂ clarity recently caught the authors' attention due to several brownish orange inclusions. These tiny crystals, only a few nanometers in size, were concentrated along two fractures in the stone (figure 11). They were identified using Raman spectroscopy as hematite (Fe₂O₃). Although it is common to find oxide staining within fractures in diamond, crystalline oxide inclusions such as these are a rarity. The concentration of the hematite crystals along the cracks suggests that, rather than being syngenetic inclusions, these are secondary (epigenetic) minerals. They likely precipitated inside the fractures when the diamond interacted with fluids while being stored in the crust. This rare sight offers a glimpse into the long and unique journey each diamond takes to the earth's surface.

Abadie Ludlam, Tingyen Yeh, and David Kondo
GIA, New York

Hyalite with Magnificent Internal Features

The Laboratoire Français de Gemmologie (LFG) received for analysis a 1.83 ct hyalite, also known as opal-AN: an amorphous (A) opal containing hydrated silica molecules that are network forming (N) (E. Fritsch et al., "Green-luminescing hyalite opal from Mexico," *Journal of Gemmology*, Vol. 34, No. 5, 2015, pp. 490–508). This is one of the

rarest varieties of gem-quality opal. The gem fluoresced green under long-wave ultraviolet (365 nm) and, with more intensity, under short-wave UV (254 nm), due to U⁶⁺ in the form of uranyl (UO₂)²⁺ (E. Gaillou et al., "Luminescence of gem opals: A review of intrinsic and extrinsic emission," *Australian Gemmologist*, Vol. 24, No. 8, 2011, pp. 200–201). A purple fluorite (identified by a micro-Raman spectrometer; figure 12) and a series of cube-shaped cavities were visible (figure 13) in the hyalite, which appear to be all interconnected. Sometimes these cavities also contain small crystals of fluorite relics detected by Raman. Thus, these cavities may be the result of the partial dissolution

Figure 12. Purple fluorite cube, identified by micro-Raman spectroscopy, in a hyalite. Photomicrograph by U. Hennebois; field of view 1.2 mm.

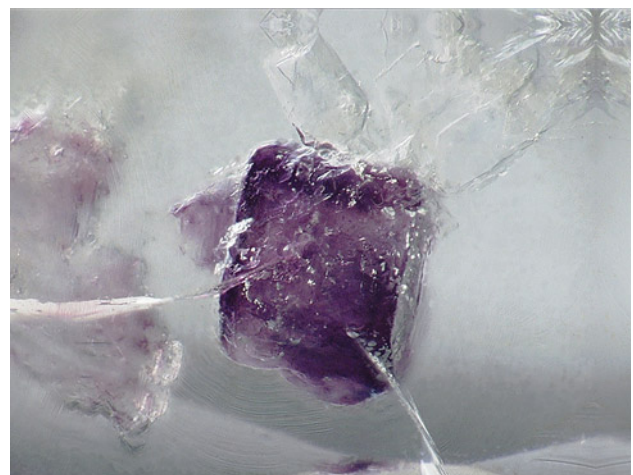




Figure 13. Interconnected cavities observed in a hyalite containing partially dissolved fluorite relics identified by Raman spectroscopy. Curved growth layers are also observed in the background. Photomicrograph by A. Delaunay; field of view 2 mm.



Figure 14. This fluid inclusion contains mostly a gaseous phase. It is trapped at the intersection of curved botryoidal growth zones and presents high-order interference colors obvious between crossed polarizers. Photomicrograph by U. Hennebois; field of view 1 mm.

of fluorite crystals. This would explain their cubic morphology, which cannot be explained by the dissolution of amorphous hyalite.

Between crossed polarizers, high-order interference colors were observed (figure 14), as expected for this gem. This is due to anomalous birefringence linked with the strain present between the curved growth layers of hyalite. Also, a fluid inclusion was observed in the intersection of the botryoids (again, see figure 14). This inclusion is composed mostly of gas, suggesting that this hyalite was deposited from a gaseous phase. Although some of these features have been previously observed in hyalite, it is rare to see them all in the same sample. To the best of our knowledge, this is the first reporting of pronounced cubic cavities in hyalite.

*Ugo Hennebois, Aurélien Delaunay, and
Stefanos Karampelas (s.karampelas@lfg.paris)
LFG, Paris*

*Emmanuel Fritsch
University of Nantes, CNRS-IMN, France*

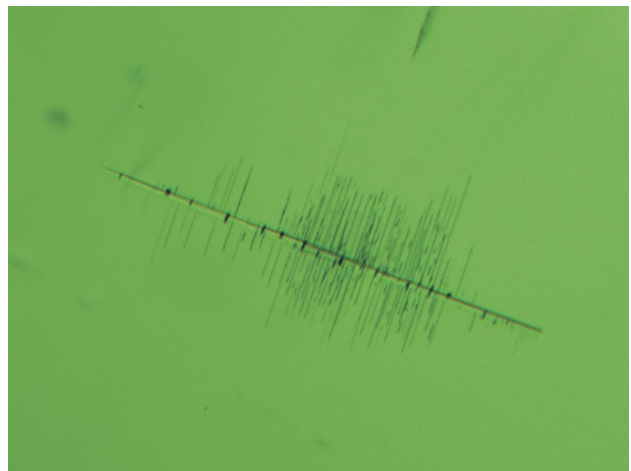
“Fishbone” Inclusion in a Burmese Peridot from Mogok

Recently, an 83.25 ct cushion faceted peridot with medium dark yellowish green color and good clarity was sent to the Taiwan Union Lab of Gem Research (TULAB) for identification service. This peridot, reported by the owner as from Mogok, Myanmar, was relatively rare in the Taiwanese market because of its impressive size, color, and clarity. Microscopic examination revealed a few short needle inclusions and a fishbone-shaped inclusion (figure 15), the latter of which is common in peridot from this origin. The

backbone appeared to be a long prismatic crystal with some vertical cleavage planes along it, while the smaller branches were composed of parallel tabular inclusions that might result from epitaxial exsolution. Due to peridot’s strong birefringence, brightfield illumination and plane polarized light were adopted to reduce the interference and obtain clear microscopic images.

*Shu-Hong Lin
Institute of Earth Sciences,
National Taiwan Ocean University
Taiwan Union Lab of Gem Research, Taipei*

Figure 15. The fishbone-like inclusion in the Burmese peridot. Photomicrograph by Shu-Hong Lin; field of view 1.32 mm.



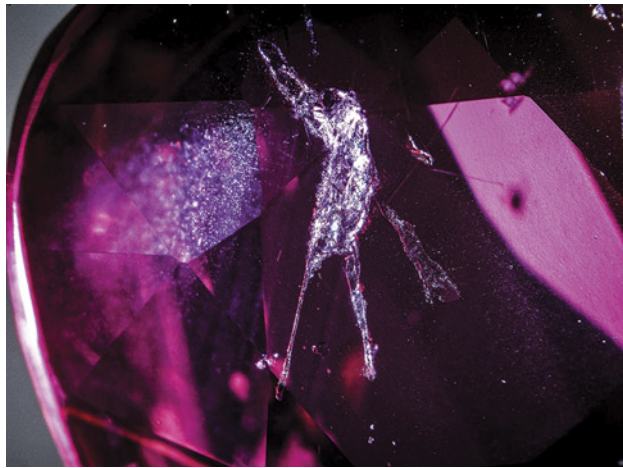


Figure 16. An extraterrestrial-like inclusion with iridescent color observed in a Mozambique ruby using fiber-optic illumination. Photomicrograph by Nattapat Karava; field of view 6.3 mm.

Extraterrestrial-Like Inclusion in Mozambique Ruby

A 3.03 ct stone submitted to GIA's Bangkok laboratory was identified as a ruby from Mozambique with no indication of heating. Microscopic examination revealed a hypnotizing inclusion that resembled an extraterrestrial standing among specks of nebulae and waving its hand (figure 16). It had a large head and very thin legs, with two

outstretched hands. This large, eye-visible inclusion was a colorless crystal among the particulate clouds. It showed iridescent color using fiber-optic illumination and was identified by Raman analysis as mica. Mica inclusions in Mozambique rubies usually have a pseudo-hexagonal shape with fringes (small expansion fractures) and can be found with a rosette pattern around them ("Rubies from the Montepuez area [Mozambique]," *GIA Research News*, 2013). This is another example of pareidolia observed in gems, the tendency to interpret an inclusion as some other object.

Nattapat Karava

An A-maze-ing Fingerprint in Spinel

Of the variety of inclusions that can be seen in spinel, perhaps the most familiar are angular octahedral crystals. In many cases, we even see these crystals arranged in neat rows, forming delicate "fingerprint" inclusions.

However, spinel fingerprints can also take on other appearances, as observed in a Vietnamese sample that recently passed through our laboratory (figure 17). This stone contained a partially healed fissure with a maze-like pattern that was evident when lit with darkfield illumination. With the addition of diffuse fiber-optic illumination, small angular areas of the channels seemed to light up with a highly reflective appearance. Myriad inclusion scenes make spinel a fascinating gem to observe.

E. Billie Hughes



Figure 17. A web-like fingerprint creates a maze-like pattern in this spinel from Vietnam, observed with darkfield and diffuse fiber-optic illumination. Photomicrograph by E. Billie Hughes; field of view 5 mm. Courtesy of Vitalit Gems.

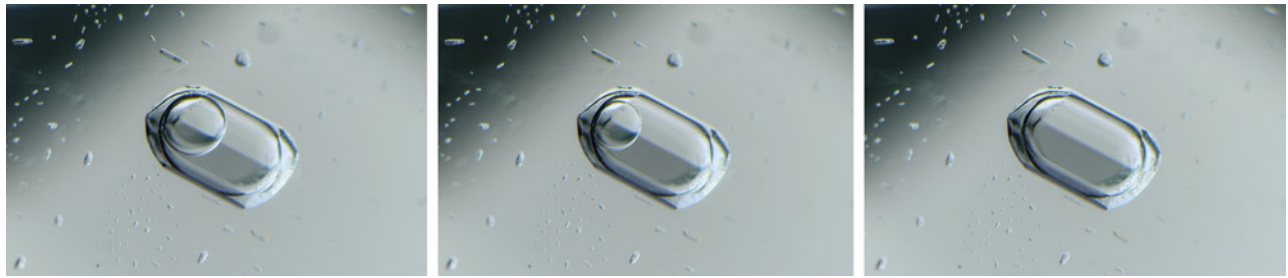


Figure 18. This complex fluid inclusion in topaz is composed of minute solid crystals, an aqueous liquid, and an immiscible CO₂ fluid. When cooled below 31.5°C, the CO₂ is in a liquid state with a vapor bubble trapped in the CO₂ liquid (left). When gently warmed, the CO₂ vapor bubble shrinks (center) until it ultimately disappears (right) as the CO₂ is homogenized into a single phase. Photomicrographs by Nathan Renfro; field of view 1.93 mm.

Complex Fluid Inclusion in Topaz

A blue topaz recently examined by the authors contained an interesting and complex fluid-filled negative crystal that revealed some remarkable behavior when cooled down. The contents of this three-phase fluid inclusion were very small solid phases, and carbon dioxide fluid trapped within an aqueous immiscible liquid, which has been previously documented (E.J. Gübelin and J.I. Koivula, *Photoatlas of Inclusions in Gemstones, Volume 2*, Opinio Verlag, Basel, Switzerland, 2005, p. 731). When the stone was cooled below approximately 31.5°C, the carbon dioxide fluid turned into liquid and gaseous states consisting of a multitude of tiny vapor bubbles nucleating and coalescing into a single larger bubble of gaseous CO₂ within the liquid CO₂ (see the video at www.gia.edu/gems-gemology/spring-2022-microworld-complex-fluid-inclusion-topaz). This type of complex inclusion results in a CO₂ vapor bubble trapped within a liquid CO₂ bubble that is trapped within an aqueous, immiscible liquid (figure 18, left). If the stone is warmed above 31.5°C, the liquid and gaseous CO₂ phases are homogenized into a single-phase fluid, causing the vapor bubble to shrink (figure 18, center) and ultimately disappear (figure 18, right). Similar behavior of CO₂ trapped in negative crystals has been previously documented in sapphire (Spring 2016 *G&G Micro-World*, pp. 78–79). The extraordinary behavior of this fluid inclusion in topaz is a delight for any gemologist.

Nathan Renfro and John I. Koivula
GIA, Carlsbad

Vietnamese Skyline

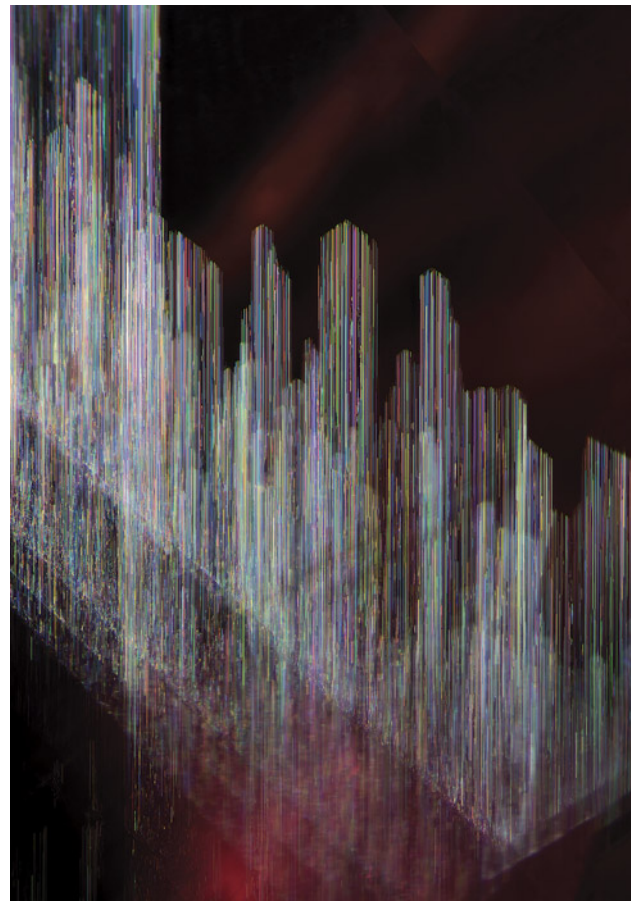
In the red spinel from Vietnam's Luc Yen district in figure 19, layers of iridescent needles stretch skyward like a futuristic skyline from a science fiction novel. Such hogbomite-filled dislocations are a common sight in red, pink, and blue spinel from Vietnam. According to Gübelin and Koivula (*Photoatlas of Inclusions in Gemstones, Volume 2*, Opinio Verlag, Basel, Switzerland, 2005), hogbomite (Mg,Fe)₂(Al,Ti)₅O₁₀ is found in spinel via isomorphous replacement.

Wimon Manerotkul
Lotus Gemology, Bangkok

YAG with Flux-Filled Fingerprints

The author recently examined a 3.58 ct yellowish green yttrium aluminum garnet, a manufactured product known in the trade as "YAG," that contained numerous large flux-filled fractures. The flux material crystallized

Figure 19. Hogbomite-filled dislocations in a Vietnamese spinel. Photo by Wimon Manerotkul; vertical field of view 4 mm.



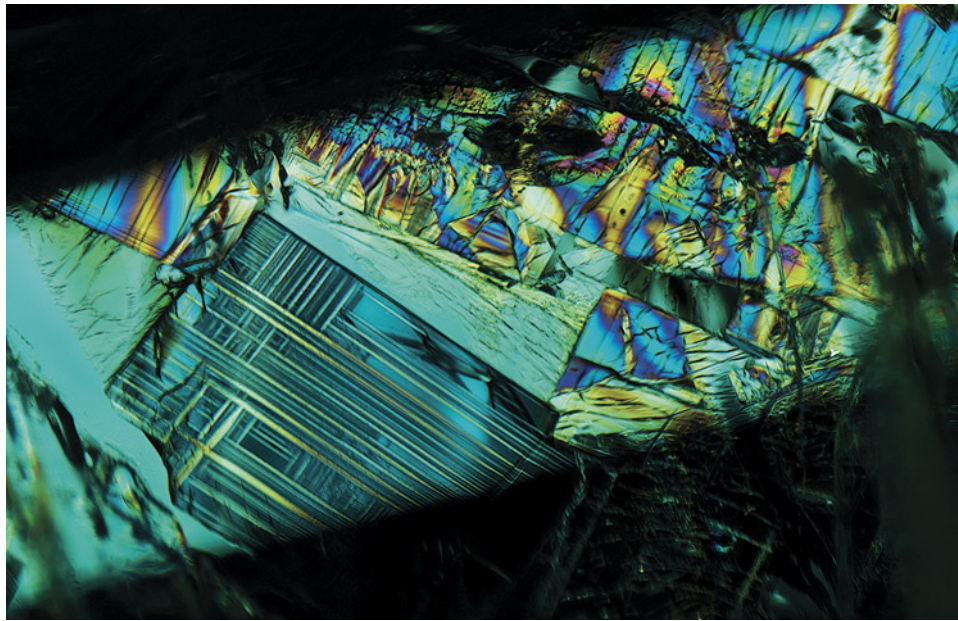


Figure 20. Flux-filled fractures displaying geometric shapes and iridescent colors when viewed through crossed polarizers. Photomicrograph by Michaela Stephan; field of view 2.9 mm.

in the fractures formed interesting geometric shapes that showed birefringent interference colors when viewed between crossed polarizers, reminiscent of stained glass windows (figure 20). It is possible this YAG was intentionally fractured and filled with flux to more convincingly imitate tsavorite grossular garnet. Although the flux inclusions in this example were quite beautiful, such inclusions are not common in this manufactured gem material.

*Michaela Stephan
GIA, Carlsbad*

Quarterly Crystal: Hillocks on Beryl

Whenever we study natural uncut gem minerals, we carefully examine all outer surfaces for any photogenic etch figures or growth hillocks that might yield interesting and educational photographs. For this issue's Quarterly Crystal, we recently had the opportunity to study a very well-formed, gem-quality aquamarine crystal supplied by Ali Shad of Shad Fine Minerals in Gilgit-Baltistan, Pakistan. The aquamarine, pictured in figure 21, was reportedly from the Qandahar mine, located in the Braldu Valley, Shigar District, Gilgit-Baltistan, Pakistan.



Figure 21. Measuring 22.28 mm in length and weighing 31.06 ct, the outer pinacoidal surface of this Pakistani aquamarine crystal is decorated with numerous hexagonal growth hillocks. Photo by Nathan Renfro.



Figure 22. The generally uniform size of the numerous growth hillocks on the terminal pinacoid of the aquamarine is clearly shown in this shadowed reflected light image. The bright colors result from light interacting with thin-film separations in the body of the aquamarine. Photomicrograph by Nathan Renfro; field of view 7.97 mm.

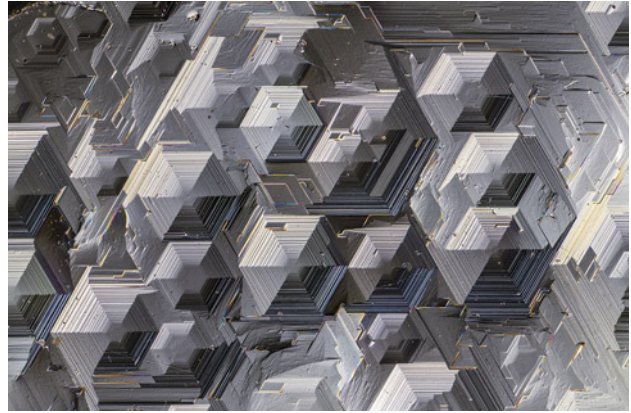


Figure 23. The complexity of some of the hexagonal growth hillocks on the pinacoid of the aquamarine is shown in closer detail in this differential interference contrast image. Photomicrograph by Nathan Renfro; field of view 2.32 mm.

At 31.06 ct with corresponding measurements of $22.28 \times 14.50 \times 11.24$ mm, this aquamarine did not show etch figures on any of its crystal faces, proving that the beryl had not gone through post-growth dissolution. However, examination showed that the pinacoid was completely covered with small hexagonal growth hillocks (figure 22) of the type discussed by John Sinkankas in *Emerald and Other Beryls* (1981) and illustrated on page

273. The hillocks on the terminal pinacoid, which were all generally of the same small size, blanketed the termination completely. Under high magnification, the hexagonal hillocks appeared very complex in form (figure 23). Their sharp, pristine, geometric habit once again illustrated that post-growth dissolution of this crystal had not taken place.

John I. Koivula and Nathan Renfro

Complex Fluid Inclusion in Topaz

To see video of a topaz containing a remarkable complex fluid inclusion, go to www.gia.edu/gems-gemology/spring-2022-microworld-complex-fluid-inclusion-topaz or scan the QR code on the right.

